

## CHAPTER 197

### Analysis on the Interaction of Waves with Flexible Floating Structure by BE-FE Combined Method

Xiaodong Liu <sup>1</sup> and Shigeki Sakai <sup>2</sup>

#### Abstract

A numerical method is developed to analyze the dynamic responses of large-scale floating structures to waves. A boundary element method is applied to evaluate the fluid motion and a finite element method to analyze the response of structure. The BEM and FEM are combined to solve the wave-structure interaction problem by satisfying the continuity of the pressure and displacement on the fluid-structure interface. The unknown time-dependent boundary conditions on the free surface and the interface are evaluated by a time-stepping procedure, which gives a time domain solution. An implicit scheme ensures the calculation precision.

#### 1. Introduction

In the analysis of floating structure, the dynamic responses of structure to waves are the most important factor. A small-scale floating structure can be analyzed as a rigid body. However, for a large-scale floating structure like floating pier, floating bridge or floating airport, the elastic deformation can not be ignored, and then the effect of flexibility should be considered in the wave-structure interaction.

In the previous studies, the wave-induced deformation of floating structure is calculated by the radiation-diffraction theory, in which the velocity potentials are expressed as a linear summation of incident, radiation and diffraction waves. This theory is available for the

---

1 Graduated Student, Dept. of Civil and Environmental Eng., Iwate University, 4-3-5 Ueda, Morioka, 020 Japan  
2 Associate Professor, Dept. of Civil and Environmental Eng., Iwate University, 4-3-5 Ueda, Morioka, 020 Japan

analysis of periodic waves, however it is difficult to solve the problem with non-periodic waves, such as the random waves in actual seas. In the present study, a numerical approach is developed to simulate the interaction of floating structure with arbitrary waves.

In order to examine the validity and applicability of the proposed numerical implementation, the calculated results are compared with experimental data.

**2. Numerical analysis**

**2.1 Governing equation and boundary conditions**

The coordinate system of two-dimensional numerical flume is defined in Figure 1. The water depth is uniform. The waves generated on the wave maker boundary propagate in  $x$  direction, and pass through under the elastic structure, which is floating on water surface and can move freely in the vertical direction. A numerical wave filter is set up on the other end of water flume to absorb the waves. The property of fluid and the condition on fluid-structure interface are assumed as follows: (1)the fluid is incompressive and inviscid; (2)the flow is irrotational; (3)structure moves with fluid inseparably and satisfies both of the Bernoulli's equation and the bending equation of structure.

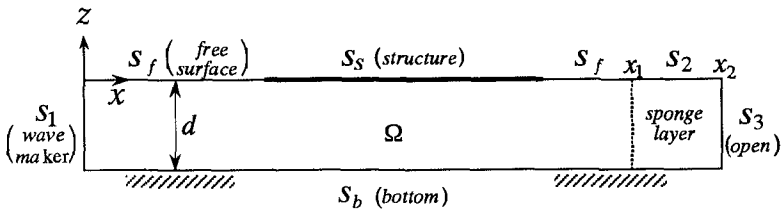


Figure 1. Definitions

According to assumption (2), a velocity potential  $\phi$  will satisfy the following governing equation in the domain  $\Omega$ :

$$\frac{\partial^2 \phi}{\partial x^2} + \frac{\partial^2 \phi}{\partial z^2} = 0 \quad \text{in } \Omega \quad (1)$$

Assuming that the waves excited on free surface is of small amplitude, the boundary conditions can be described as

$$\frac{\partial \phi}{\partial x} = V_n \quad \text{on } S_1 \quad (2)$$

$$\frac{\partial \phi}{\partial n} = 0 \quad \text{on } S_b \quad (3)$$

$$\frac{\partial \phi}{\partial n} = \frac{\partial z}{\partial t} \quad \text{on } S_f, S_s, S_2 \quad (4)$$

$$\frac{\partial \phi}{\partial t} + gz + \frac{p}{\rho} = 0 \quad \text{on } S_f, S_s \quad (5)$$

$$\frac{\partial \phi}{\partial t} + gz + \mu \phi - \int_{x_1}^x \phi \frac{\partial \mu}{\partial x} dx = 0 \quad \text{on } S_2 \quad (6)$$

$$\frac{\partial \phi}{\partial x} = -\frac{1}{\sqrt{gd}} \frac{\partial \phi}{\partial t} \quad \text{on } S_3 \quad (7)$$

where,  $t$  is time and  $n$  means the outward normal direction on boundary. (2) gives the water particle velocity of waves generated on wave maker boundary, and (3) is the impermeability condition on bottom boundary. (4) and (5) are the kinematic and dynamic conditions on the free surfaces and the interface. (6) is the dynamic condition on the free surface of the wave filter and (7) is the Sommerfeld equation on the outside boundary of the wave filter.

## 2.2 Boundary integral equations

As the velocity potential  $\phi$  is a harmonic function, the Laplace equation in domain  $\Omega$  can be derived as the boundary integral equation by using Green's equation.

$$c^*(\chi_l)\phi(\chi_l) = \int_{s(\chi)} \left[ \frac{\partial \phi(\chi)}{\partial n} G(\chi, \chi_l) - \phi(\chi) \frac{\partial G(\chi, \chi_l)}{\partial n} \right] ds \quad (8)$$

$$G(\chi, \chi_l) = -\frac{1}{2\pi} \log|\chi - \chi_l|$$

where,  $\chi = (x, z)$  and  $\chi_l = (x_l, z_l)$  are the position vector on boundaries at the points of consideration and application respectively, and  $c(\chi_l)$  is the parameter corresponding to the configuration of boundaries.

By substituting (2), (3), (4) and (7) into (8), the

relation between the unknowns of the velocity potential  $\phi$  on all boundaries and the variable  $z$  on the free surface and the interface can be expressed by the following integral formulation.

$$c^*(\chi_l)\phi(\chi_l) = -\int_S \phi \frac{\partial G}{\partial n} ds + \int_{S_f, S_s, S_2} \frac{\partial z}{\partial t} G ds + \int_{S_1} V_n G ds + \int_{S_3} \left( \frac{\partial \phi}{\partial x} \right) G ds \quad (9)$$

On the right side of the above equation, the third term is known by giving the normal water particle velocity of waves on wave maker boundary. The fourth term is treated by the transformed Sommerfeld condition on the outside boundary of wave filter, which will be explained in part 2.4. The second term is the unknown time-dependent part including free surfaces and structure surface. To obtain the solution that satisfies equation (9), it is necessary to utilize the dynamic boundary conditions.

The dynamic boundary condition on free surface  $S_f$  is described by imposing  $p=0$  into equation (5)

$$\frac{\partial \phi}{\partial t} + gz = 0 \quad \text{on } S_f \quad (10)$$

where  $z$  is the displacement measured from the equilibrium water surface.

The dynamic boundary condition on the free surface of wave filter is shown in equation (6). If  $\mu = \partial \mu / \partial x = 0$ , it will be identical with the general form, like equation (10).

The dynamic condition on structure surface is introduced in part 2.3 in detail.

### 2.3 Finite element analysis of structure

The flexible floating structure is considered as a plate with unit width, in which the effect of axis force is neglected. By discretizing the continuous body into elements, and converting the distribution force acting on each element into the concentrated force acting on the nodal points, the finite element analysis can give the solution of structure deformation from the dynamic condition on fluid-structure interface by satisfying the continuity of the nodal displacement.

The dynamic equilibrium equations for a finite element

system in motion can be written in matrix form

$$[M]\ddot{\{V\}} + ([K] + [K_d])\{V\} = \{F\} \quad (11)$$

where,  $[M]$ : the assembled mass matrix of structure  
 $[K]$ : the assembled stiffness matrix  
 $[K_d]$ : the converted coefficient matrix of the hydrostatic restoring force  
 $\{V\}$ : the displacement vector  
 $\{F\}$ : the external force vector

The mass matrix and stiffness matrix are calculated by the general approach of finite element method. The hydrostatic restoring force ( $\rho g v(x)$ ), which is proportional to the displacement  $v(x)$  of structure, is a distribution force along elements. By changing the distribution force into the equivalent concentrated forces at nodal points, the coefficient terms corresponding to the displacement can be described in the form of the element coefficient matrix  $[K_d]^e$ , which is

$$[K_d]^e = \frac{\rho g l}{420} \begin{bmatrix} 156 & 22l & 54 & -13l \\ 22l & 4l^2 & 13l & -3l^2 \\ 54 & 13l & 156 & -22l \\ -13l & -3l^2 & -22l & 4l^2 \end{bmatrix} \quad (12)$$

where,  $\rho$  is water density,  $g$  is the acceleration due to gravity, and  $l$  is the length of element. The coefficient matrix of the complete element assemblage is obtained by the direct addition of the element coefficient matrices similar to the assemblage of stiffness matrix.

Moreover, the fluid pressure ( $p = -\partial\phi/\partial t$ ) that acts on floating body is a distribution force varying with the velocity potentials. It is also needed to convert the distribution force into the equivalent concentrated forces at nodal points. And then, the external force vector  $\{F\}$  can be obtained by adding the nodal forces to the corresponding points.

In dynamic analysis, the equilibrium equations (11) are solved by using the Newmark integration scheme.

#### 2.4 Wave filter boundary condition

In order to decrease the reflection waves from the far end of flume, a numerical wave filter proposed by Ohyama et al(1985) is employed to absorb the waves. The numerical wave filter consists of a sponge layer for absorbing the energy of incident waves and a Sommerfeld boundary for radiating the incoming waves. The sponge layer can be effectively used to absorb the component waves within a wide period range. But if the wave length is larger than the width of sponge layer, the efficiency of the sponge layer decreases. Therefore, the Sommerfeld condition applied on the outside boundary of the sponge layer can absorb the wave energy of long period waves.

Assuming that the attenuation coefficient  $\mu$  in the sponge layer distributes linearly in horizontal direction and imposing eq.(6) to eq.(7), the boundary condition on  $S_3$  that satisfies the continuity of velocity and pressure can be derived as follow

$$\frac{\partial \phi}{\partial x} = -\frac{1}{\sqrt{gd}} \left( \frac{\partial \phi}{\partial t} + \mu \phi - \int_{x_1}^{x_2} \phi \Big|_{on S_2} \frac{\partial \mu}{\partial x} dx \right) \quad \text{on } S_3 \quad (13)$$

## 2.5 Time-stepping procedure

The velocity potential  $\phi$  on the discrete nodal points along all the boundaries and the nodal displacements on free surface and fluid-structure interface are time-defendant variables. The time under consideration is subdivided into the constant time intervals  $\Delta t$ , the motions of fluid and floating body can be described by a time-stepping scheme, in which a solution is established at each time step. Assuming that the velocity potential and its time derivatives at time  $t$ , denoted by  $\phi^k, \dot{\phi}^k$  and  $\ddot{\phi}^k$ , respectively, are known, and that  $\phi^{k+1}, \dot{\phi}^{k+1}$  and  $\ddot{\phi}^{k+1}$  at time  $t+\Delta t$  are unknown, the relation of the unknowns at time step  $k+1$  and the knowns at time step  $k$  on nodal point  $i$  can be expressed by the constant-average-acceleration scheme, as follow.

$$\phi_i^{k+1} = \phi_i^k + \Delta t \dot{\phi}_i^{k+1} = \phi_i^k + \Delta t \dot{\phi}_i^k + \frac{\Delta t^2}{4} (\ddot{\phi}_i^k + \ddot{\phi}_i^{k+1}) \quad (14)$$

$$\dot{\phi}_i^{k+1} = \frac{2}{\Delta t} (\phi_i^{k+1} - \phi_i^k) - \dot{\phi}_i^k \quad (15)$$

$$\ddot{\phi}_i^{k+1} = \frac{4}{\Delta t^2} (\phi_i^{k+1} - \phi_i^k) - \frac{4}{\Delta t} \dot{\phi}_i^k - \ddot{\phi}_i^k \quad (16)$$

At the nodal point  $i$  on free and interface boundaries, the displacement, velocity and acceleration at step  $k+1$  can be also expressed in the similar relation equation in terms of the previous solutions.

In the time-stepping calculation employed in this paper, at first,  $\phi_i^{k+1}$  is predicted in relation (14), in which  $\Delta\phi_i^{k+1}$  is approximately evaluated by the solution of the previous time step in relation (17).

$$\Delta\phi_i^{k+1} \approx \Delta t \dot{\phi}_i^k + \frac{\Delta t^2}{2} \ddot{\phi}_i^k \quad (17)$$

And then, the vertical velocity and displacement on free surface and interface are calculated from the boundary integration equation (9). The velocity potential  $\phi_i^{k+1}$  required can be evaluated by the dynamic conditions of eq.(6),(10) and (11). For one step's calculation, it repeats until the relative error between  $\phi_i^{k+1}$  evaluated and that predicted is smaller than a given value. The solution is given by an implicit method.

### 3. Calculated and experimental results

#### 3.1 Experimental equipment

The wave flume used for the present experiments is 26m long, 0.8m wide and 1m deep, as illustrated in figure 2. The water depth is 60cm. A wave generator is placed at one end of the flume. The wave generator has an absorbing system so that any reflected waves from the floating structure will not be reflected by the paddle of the wave maker. At the other end a wave absorber is installed to decrease wave reflection. Three kinds of

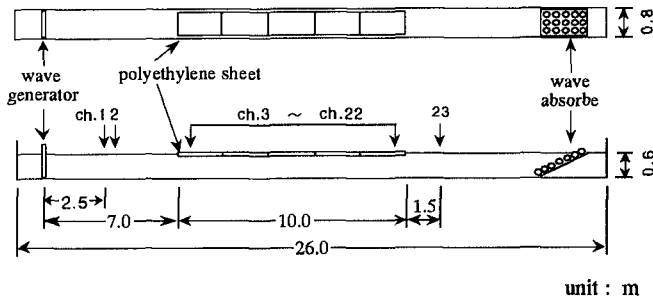


Figure 2. Experimental equipment

polyethylene plates with thickness 5mm, 10mm and 20mm are used as the model floating structure. The density of polyethylene plate is 0.941 and its elastic modulus is about 450 MPa. The wave profiles in the front open water are measured by two wave gauges. The vertical displacements of the floating body are measured at 20 points along the center of the flume by using an array of ultra-sonic sensors.

### 3.2 The numerical wave flume

The definition of the numerical two-dimensional wave flume is shown in figure 3. In the discretization of all boundaries, the element length on floating structure is 0.1m, 0.2m on free surface and 0.5m on the bottom. The calculation starts with a still water as the initial condition, and waves are produced by giving the water particle velocity and elevation on wave maker boundary. The step-by-step calculation proceeds with the time intervals of 1/100 wave period and the relative error 0.01 for each calculation step.

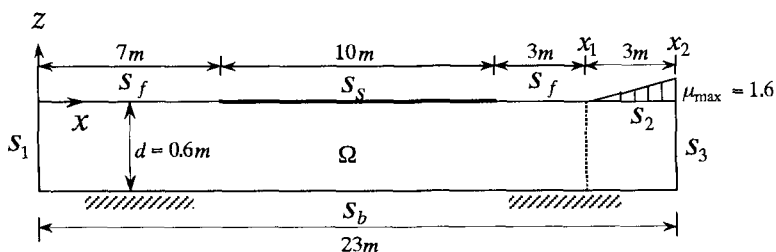


Figure 3. Definition of the numerical wave flume

### 3.3 Deformation of water surface and structure

Fig.4 shows an example of the calculated wave profile and the structure deformation at  $t=24\text{s}$  after the waves are generated from a still water condition. In this case, the structure is 20mm thick and the wave period is 1.2 second. It can be seen clearly that the wavelength under the structure increases and the wave height (structure deformation amplitude) decreases significantly.

In figure 5, the time histories of deformation at several nodal points are plotted. The top one and the bottom one are in front and rear open waters respectively, and that in the middle part are on floating structure. In this figure, the vertical axis gives the value of vertical deformation and the horizontal axis is time.



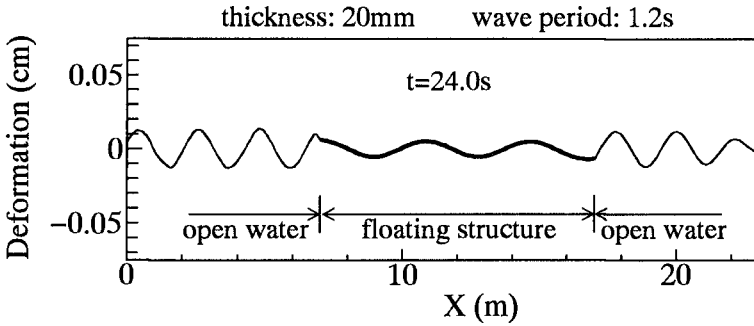


Figure 4. Deformation in open water and structure

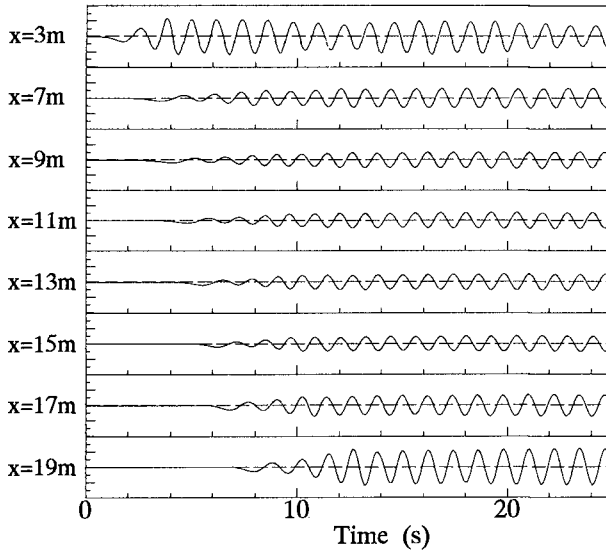


Figure 5. Time history deformation

The waves in front open water become stable, and then are influenced by the reflection waves due to the motion of floating body. For the deformation of structure, the amplitudes are large at both ends and small in structure. The motion of structure become stable after five waves pass through the structure. The variation of water surface elevation in front of wave filter is in steady state, therefore the waves are absorbed in the wave filter and the motion of floating structure is not influenced by the reflection waves.

3.4 Structure displacement response

Figure 6 shows the vertical deformation amplitude of structure with the thickness of 20mm and the wave periods of 0.8s and 1.4s. In this figure, the experimental data are the average values of wave heights measured by the time history deformation at the five waves that are in steady state. The amplitudes decrease significantly near the edge of the structure. This phenomenon is attributed to the energy conversion when the fluid motion changes into the structure-fluid combined motion. Both of the measured and the calculated results show that the deformation amplitudes exit the modes which depend on the length of structure and the period of incident waves, and they agree with each other very well.

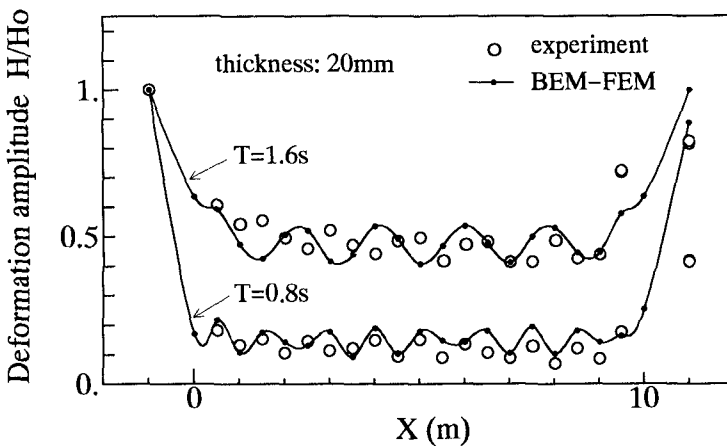


Figure 6. Deformation amplitude of structure

Figure 7 shows the changing rates of deformation amplitudes when waves propagate into structure by energy conservation method, potential matching method, the present method and experiments, respectively. The amplitude changing rates by the present method are calculated by evaluating the average amplitudes excluding the values near the edges of structure. The amplitude variations at structure edge based on the present method coincide with the measured data well.

### 3.5 Moment response

Figure 8 shows the response of bending moment for 20mm-thick floating structure. The peaks exist at several places and the mode observed depends on the incident wave periods. The longer the wave period becomes, the

lower the order of mode is and the greater the bending moment becomes.

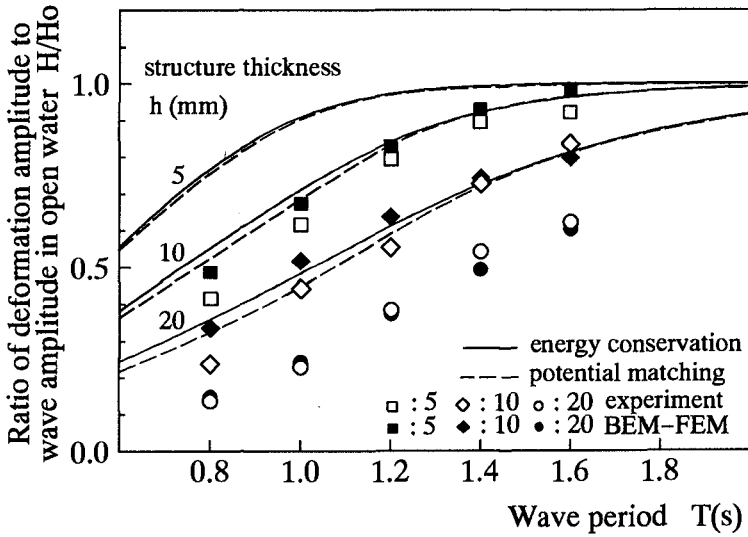


Figure 7. Comparisons of the amplitude changing rates at the edge of floating structure

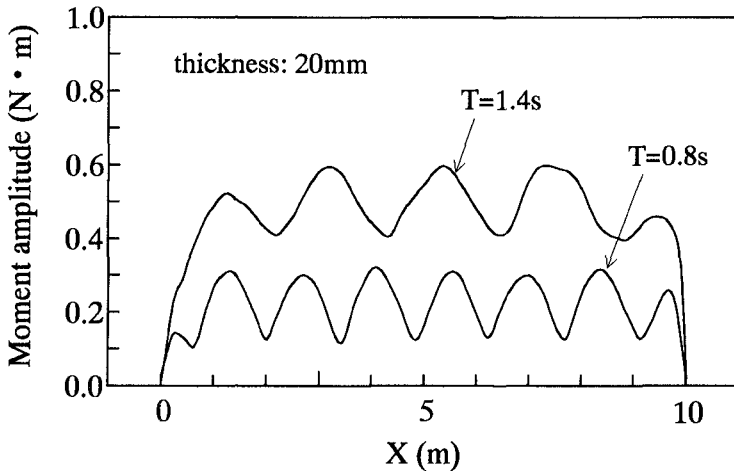


Figure 8. Moment response

#### 4. Conclusions

The numerical approach proposed in the present study simulates the interaction of waves and flexible floating structure by employing BEM for evaluating the fluid motion and FEM for calculating the deformation of floating structure. By satisfying the continuity of the pressure and displacement on the fluid-structure interface, the BEM and FEM are combined to solve the interaction problem. The proposed method is of the following advantages: (1) The dynamic responses of structure to waves are calculated in a time-stepping procedure, which gives a time-domain solution; (2) The velocity potential is not expressed by any assumed function and is evaluated numerically. Therefore, the present method can be easily applied to any wave condition including random waves just by giving the values of incident waves on the wave maker boundary of the numerical wave flume; (3) The unknown time-dependent boundary conditions on the free surface and fluid-structure interface are evaluated by an implicit predictor-corrector scheme, which ensures a calculation precision.

The comparisons between the calculated and experimental results show that the present method is effective to the dynamic response analysis of flexible floating structures to waves.

#### Reference

1. Brebbia, C.A., "The Boundary Element Method For Engineers", Pentech Press, 1980
2. Sakai, S., "Interaction of Waves and Ice", Lecture Notes of the 31st Summer Seminar on Hydraulic Engineering, 95-B-2, JSCE, 1995 (in Japanese)
3. Ohyama, T. and Nadaoka, K., "Wave-Absorbing Filter for Open Boundary in Numerical Wave Tank", Proc. of Coastal Engineering, JSCE, Vol.37(1), pp.16-20, 1990 (in Japanese)
4. Suzuki Y., Tomita, Y. and Matumori, T., "Numerical Analysis of the Movement and Transmission Coefficient of Flexible Floating Structure in Waves", Proc. of Coastal Engineering, JSCE, Vol.40(2), pp.896-900, 1993 (in Japanese)